

GAS STRIPPING OF DWARF GALAXIES IN CLUSTERS OF GALAXIES

MASAO MORI¹ AND ANDREAS BURKERT

Max-Planck-Institut für Astronomie, Königstuhl 17, D-69117 Heidelberg, Germany

accepted to the Astrophysical Journal

ABSTRACT

Many clusters of galaxies contain an appreciable amount of hot gas, the intracluster medium. As a consequence, gas will be stripped from galaxies that move through the inter cluster medium, if the ram pressure exceeds the internal gravitational force. We study the interaction between the intracluster medium and an extended gas component of dwarf galaxies confined by a surrounding cold dark matter halo analytically and numerically, using axisymmetric two-dimensional hydrodynamical simulations at high resolution. The results show that the gas within the dark matter halo is totally stripped in a typical galactic cluster. The process of ram pressure stripping therefore must have played an important role during the chemo-dynamical evolution of dwarf galaxies in galactic clusters. Our results predict that most of the chemical evolution of dwarf galaxies must have occurred at high redshift, before the virialized cluster had formed.

Subject headings: galaxies: dwarf — formation — evolution — clusters — intergalactic medium

1. INTRODUCTION

Explaining the morphology-density relation (Dressler 1980), that is the higher early-type galaxy fraction in clusters of galaxies in contrast to the higher late-type galaxy fraction in the fields, remains one of the most important problems in cosmology. This relation holds also for dwarf galaxies. Gas-poor dwarf galaxies are strongly clustered, while gas-rich dwarf galaxies appear to be the most weakly clustered objects (Binggeli et al. 1987; Ferguson & Sandage 1988; Binggeli et al. 1990; Thuan et al. 1991).

Since many clusters of galaxies contain an appreciable amount of hot gas, the intracluster medium (ICM), gas will be stripped from galaxies that move through the ICM, if the ram pressure exceeds the internal gravitational force. There are actually many observational evidences for the ram pressure stripping of giant galaxies in clusters of galaxies (Irwin et al. 1987; White et al. 1991; Böhringer et al. 1995). In addition, the physics of ram pressure stripping of giant galaxies has been studied in detail using hydrodynamic simulations (e.g. Balsara, Livio, & O’Dea 1994 and references therein). Since dwarf galaxies have smaller escape velocities, ram pressure stripping is expected to be more efficient than for giant galaxies. However, no attempts have ever been made to examine the amount of gas that could be stripped from low-mass galaxies with shallow gravitational potential wells during their passage through an ICM.

This situation motivated us to consider the ram pressure stripping of the diffuse gas phase of dwarf galaxies by the ICM which may be of prime importance to understand the morphology-density relation for dwarf galaxies. We estimate the critical condition for gas removal by the interaction between an ICM and gaseous dwarf galaxies confined by a surrounding cold dark matter (CDM) halo. Moreover, we verified that condition using an axial symmetric two-dimensional hydrodynamic code which is based on the piecewise parabolic method (PPM) described by Colella & Woodward (1984).

In §2, prior to the main subject, we describe the model of dwarf galaxies which is treated as a one-parameter family defined by the core mass of the CDM halos, using the observed scaling relation (Burkert 1995). In §3, we give the analytical estimates of the critical conditions for the gas ablation from dwarf galaxies due to ram pressure stripping by the ICM. In §4, we demonstrate the complex interaction between dwarf galaxies and the ICM using hydrodynamical simulations and compare the simulation results with the analytical predictions. In §5, we summarise the results of this paper, and discuss observational and theoretical implications.

2. MODEL OF DWARF GALAXIES

The hierarchical clustering model of galaxies has been successful in explaining the clustering pattern of galaxies revealed by redshift surveys. On the other hand, the hierarchical model predicts a large number of low-mass galaxies formed at high redshifts beyond that estimated from the observed luminosity function of galaxies (White & Frenk 1991; Cole et al. 1994). Therefore, several mechanisms for suppressing and/or delaying the formation of dwarf galaxies have been proposed in order to remove this serious discrepancy.

Using a three-dimensional N -body/SPH simulation code combined with stellar population synthesis, Mori et al. (1997) showed that an energy feedback via supernovae and stellar winds from massive stars keeps a large fraction of the gas hot and suppresses the formation of dwarf galaxies. Moreover, they pointed out that this energy feedback is a necessary mechanism to reproduce the internal structure and the photometric quantities of the nearby dwarf galaxies (see also Dekel & Silk 1986; Yoshii & Arimoto 1987; Burkert & Ruiz-Lapuente 1997; Mori, Yoshii & Nomoto 1999).

Babul & Rees (1992) and Efstathiou (1992) argued that the formation epoch of dwarf galaxies is delayed until $z < 1$ due to the photoionization of the gas by the ultraviolet

¹ Institute of Astronomy, University of Tokyo, Mitaka, Tokyo 181-8588, Japan

background radiation at high redshifts. The ionizing background at $z > 1$ is high enough to keep the gas in dwarf galaxy halos confined and stable, neither able to escape, nor able to collapse (see also Rees 1986; Ikeuchi 1986; Katz, Weinberg & Hernquist 1996; Navarro & Steinmetz 1997).

Following this scenario, we assume that a (proto-) dwarf galaxy has an already virialized CDM halo and a large amount of extended hot gas heated either due to a first population of supernovae or due to the photoionization by ultraviolet background radiation at the formation epoch of the galaxy clusters.

2.1. Structure of the CDM halos

The formation of the CDM halos through hierarchical clustering predicts that the equilibrium density profile of a CDM halo has a central cusp (Dubinski & Carlberg 1991; Navarro, Frenk & White 1996; Fukushige & Makino 1997; Moore et al. 1998). However, recent observed rotation curves of nearby dwarf galaxies rule out the singular density profile of dark matter halos (Flores & Primack 1994; Moore 1994). Moreover, Burkert (1995) points out that the density profile

$$\rho_d(r) = \frac{\rho_{d0} r_0^3}{(r + r_0)(r^2 + r_0^2)}, \quad (1)$$

nicely reproduces the rotation curves of nearby dwarf galaxies and the central density ρ_{d0} is correlated with the core radius r_0 through a simple scaling relation.

In this paper we assume that the density distribution of the CDM halos is represented by Burkert's (1995) profile for a wide range of core masses from $10^6 M_\odot$ to $10^{10} M_\odot$. For the density distribution of the CDM halo in equation (1), the potential is found by integrating Poisson's equation as

$$\begin{aligned} \Phi_d(r) = & -\pi G \rho_{d0} r_0^2 \left[\pi - 2 \left(1 + \frac{r_0}{r} \right) \arctan \frac{r_0}{r} \right. \\ & + 2 \left(1 + \frac{r_0}{r} \right) \ln \left(1 + \frac{r}{r_0} \right) \\ & \left. - \left(1 - \frac{r_0}{r} \right) \ln \left\{ 1 + \left(\frac{r}{r_0} \right)^2 \right\} \right]. \quad (2) \end{aligned}$$

The central potential is given by $\Phi_d(0) = -\pi^2 G \rho_{d0} r_0^2$, where G is the gravitational constant. The mass distribution of the CDM halo is given by

$$\begin{aligned} M_d(r) = & \pi \rho_{d0} r_0^3 \left[-2 \arctan \frac{r}{r_0} \right. \\ & \left. + 2 \ln \left(1 + \frac{r}{r_0} \right) + \ln \left\{ 1 + \left(\frac{r}{r_0} \right)^2 \right\} \right]. \quad (3) \end{aligned}$$

Using the observed scaling relation derived by Burkert (1995), ρ_{d0} and r_0 are calculated as

$$r_0 = 3.07 \left(\frac{M_0}{10^9 M_\odot} \right)^{\frac{3}{7}} \text{ kpc}, \quad (4)$$

and

$$\rho_{d0} = 1.46 \times 10^{-24} \left(\frac{M_0}{10^9 M_\odot} \right)^{-\frac{2}{7}} \text{ g cm}^{-3}, \quad (5)$$

where the core mass M_0 is the total mass of the CDM halo inside r_0 .

The circular velocity $v_c^2 = GM_d(r)/r$ of the CDM halo has a maximum value

$$v_{c,\max} = 48.7 \left(\frac{M_0}{10^9 M_\odot} \right)^{\frac{2}{7}} \text{ km s}^{-1}, \quad (6)$$

at the radius of $r_{c,\max} = 3.24 r_0$ (see Fig. 1). This velocity and the radius are related by

$$v_{c,\max} = 10.5 \left(\frac{r_{c,\max}}{\text{kpc}} \right)^{\frac{2}{3}} \text{ km s}^{-1}. \quad (7)$$

2.2. Structure of the gas

We focus on the general question of the interaction between the intracluster medium and a hot gaseous component in dwarf galaxies that is generated e.g. by the supernova heating (Dekel & Silk 1986; Burkert & Ruiz-Lapuente 1997; Mori et al. 1997; Mori et al. 1999), or by the photoionization due to the ultraviolet background radiation (Efstathiou 1992; Babul & Rees 1992). In this case the gas is pressure supported justifying the assumption of an initially spherically symmetric distribution and of axi-symmetry.

The self-gravity of the gas is neglected for simplicity and the gas is assumed to be in hydrostatic equilibrium with the constant temperature

$$T = \frac{\mu m_p G M_0}{3 k_B r_0}, \quad (8)$$

$$= 3.45 \times 10^4 \left(\frac{M_0}{10^9 M_\odot} \right)^{\frac{4}{7}} \text{ K}, \quad (9)$$

where μ is the mean molecular weight, m_p is the proton mass, and k_B is the Boltzmann's constant. The density distribution of the gas is given by

$$\rho_g(r) = \rho_{g0} \left[-\frac{\mu m_p}{k_B T} \{ \Phi_d(r) - \Phi_d(0) \} \right], \quad (10)$$

where ρ_{g0} is the central density of the gas. The mass ratio between the gas and the CDM halo within a core radius is defined as

$$F = \frac{M_{g0}}{M_0}, \quad (11)$$

where M_{g0} is the total gas mass inside a core radius. The relation between the central density of the gas and of the dark matter is given by the numerical solution of equation (11): $\rho_{g0} = 1.40 F \rho_{d0}$. We assumed initially $F = 0.1$ in this paper. Consequently each dwarf galaxy is described as a one-parameter family by the core mass M_0 of the CDM halos.

3. ANALYTICAL MODEL

The stripping process is generally classified into two distinct types such as the instantaneous stripping phase and the continuous stripping phase due to Kelvin-Helmholtz instability. In this section, we estimate analytically the gas ablation affects on the evolution of a dwarf galaxy.

3.1. Instantaneous ram pressure stripping

We assume that the CDM halo associated with the dwarf galaxies moves in a homogeneous ICM with number density of $n_{CG} = \rho_{CG}/(\mu m_p) \sim 10^{-4} \text{ cm}^{-3}$ and relative velocity $v_{gal} \sim 10^3 \text{ km s}^{-1}$ corresponding to the three-dimensional velocity dispersion of the galaxy cluster.

The complete condition for the ram pressure stripping from a dwarf galaxy requires that the ram pressure of the ICM exceeds the thermal pressure $\rho_{g0} k_B T / (\mu m_p)$ at the center of the gravitational potential well of the CDM halo. Using equation (8), such a condition is described by

$$\rho_{CG} v_{gal}^2 > \frac{GM_0 \rho_{g0}}{3r_0}. \quad (12)$$

Thus, if the core mass M_0 is smaller than the critical core mass

$$M_{IS} = 1.27 \times 10^9 \left(\frac{F}{0.1} \right)^{-\frac{7}{2}} \left(\frac{n_{CG}}{10^{-4} \text{ cm}^{-3}} \right)^{\frac{7}{2}} \times \left(\frac{v_{gal}}{10^3 \text{ km s}^{-1}} \right)^7 M_{\odot}, \quad (13)$$

the gas in a dwarf galaxy is totally stripped by the ram pressure of the ICM.

The collision between the gas of the dwarf galaxy and the ICM generates a forward shock that propagates through the gas of the dwarf galaxy and a reverse shock that propagates through the ICM. The time-scale of the gas removal is roughly estimated by dividing the diameter of the core by the velocity of the forward shock v_{fs} . The analysis of the one-dimensional shock problem gives

$$v_{fs} = \frac{4}{3} \sqrt{\frac{\rho_{CG}}{\rho_{g0}}} v_{gal}, \quad (14)$$

for the high-speed collision of two homogeneous non-gravitating media with large density ratio ($\rho_{CG} \ll \rho_{g0}$). The time-scale of the mass removal from dwarf galaxies is estimated by

$$\begin{aligned} \tau_{IS} &= \frac{2r_0}{v_{fs}}, \quad (15) \\ &= 2.02 \times 10^8 \left(\frac{F}{0.1} \right)^{\frac{1}{2}} \left(\frac{M_0}{10^9 M_{\odot}} \right)^{\frac{2}{7}} \\ &\quad \times \left(\frac{n_{CG}}{10^{-4} \text{ cm}^{-3}} \right)^{-\frac{1}{2}} \left(\frac{v_{gal}}{10^3 \text{ km s}^{-1}} \right)^{-1} \text{ yr} \end{aligned} \quad (16)$$

Consequently, the gas is totally stripped from less-massive dwarf galaxies ($M_0 \lesssim 10^9 M_{\odot}$) in the typical environment of the ICM because the ram pressure of the ICM exceeds the gravitational force of these galaxies. The time-scale of the gas removal is small compared with the characteristic time-scale (several Gyr) a galaxy spends within potentials, therefore, lose their gas easily within this dwarf galaxies ($M_0 \gtrsim 10^9 M_{\odot}$) the gas might be significantly removed except around the central region of the gravitational potential well.

3.2. Kelvin-Helmholtz instability

Gas in the massive dwarf galaxies surviving the instantaneous ram pressure stripping is subsequently removed by Kelvin-Helmholtz instability occurring at the interface between the gas in the dwarf galaxy and the ICM. Murray et al. (1993) estimated the characteristic growth time of Kelvin-Helmholtz instability for a dense cloud embedded in a low-density background. They showed that the growth time is comparable to the sound crossing time of the gas cloud if gravity is negligible. On the contrary, the presence of a gravitational field by the surrounding CDM halo tends to suppress the instability and to stabilize the gas against removal from the dwarf galaxy.

We suppose that the process of the instantaneous ram pressure stripping removes the gas distributed outside a core radius r_0 . Moreover, a sharp discontinuity of the gas density is established between the ICM and the galactic gas having nearly constant density after the shock passage. The unstable wave number of Kelvin-Helmholtz instability at the interface for the incompressible fluid is given by

$$k > g \frac{\rho_{CG}^2 - \rho_{g,avg}^2}{\rho_{CG} \rho_{g,avg} v_{gal}^2}, \quad (17)$$

where $\rho_{g,avg}$ is the mean gas density inside r_0 and $g = GM_0/r_0^2$ is the gravitational acceleration at the fluid interface (cf. Chandrasekhar 1961). Since the dominant wavelength for the gas ablation by Kelvin-Helmholtz instability is the order of r_0 (Murray et al. 1993), the inequality (17) for $\rho_{CG} \ll \rho_{g,avg}$ is transformed as

$$\rho_{CG} v_{gal}^2 > \frac{GM_0 \rho_{g,avg}}{2\pi r_0}. \quad (18)$$

Using this inequality, it is found that the diffuse gas component in these galaxies is removed if their core mass M_0 does not exceed a critical value given by

$$M_{KH} = 1.60 \times 10^{12} \left(\frac{F}{0.1} \right)^{-\frac{7}{2}} \left(\frac{n_{CG}}{10^{-4} \text{ cm}^{-3}} \right)^{\frac{7}{2}} \times \left(\frac{v_{gal}}{10^3 \text{ km s}^{-1}} \right)^7 M_{\odot} \quad (19)$$

This value corresponds to masses characteristic for a giant galaxy which indicates that dwarf galaxies should in general be affected by Kelvin-Helmholtz stripping. The gas ablation due to Kelvin-Helmholtz instability is effective for massive dwarf galaxies if the mass-loss time-scale is smaller than the characteristic time-scale a galaxy spends within a cluster environment.

According to Nulsen (1982) the mass-loss rate from the galaxy through Kelvin-Helmholtz instability is estimated as

$$\dot{M}_{KH} = \pi r_0^2 \rho_{CG} v_{gal}, \quad (20)$$

the gas removal time-scale of the dwarf galaxies is therefore given by

$$\tau_{KH} = \frac{FM_0}{\dot{M}_{KH}}, \quad (21)$$

$$= 2.19 \times 10^9 \left(\frac{F}{0.1} \right) \left(\frac{M_0}{10^9 M_{\odot}} \right)^{\frac{1}{7}} \left(\frac{n_{CG}}{10^{-4} \text{ cm}^{-3}} \right)^{-1} \times \left(\frac{v_{gal}}{10^3 \text{ km s}^{-1}} \right)^{-1} \text{ yr}. \quad (22)$$

TABLE 1
PARAMETERS OF THE ICM

Model	n_{CG} cm^{-3}	v_{gal} km s^{-1}	T_{CG}^a K	M^b	$\rho_{CG} v_{gal}^2$ erg cm^{-3}
(a)	1.0×10^{-3}	1000	1.0×10^7	2.1	1.0×10^{-11}
(b)	1.0×10^{-3}	500	1.0×10^7	1.1	2.6×10^{-12}
(c)	1.0×10^{-4}	1000	1.0×10^7	2.1	1.0×10^{-12}
(d)	1.0×10^{-4}	500	1.0×10^7	1.1	2.6×10^{-13}
(e)	1.0×10^{-5}	1000	1.0×10^7	2.1	1.0×10^{-13}

^aTemperature of the ICM

^bMach number of the ICM

Moreover, it should be noted that the characteristic time-scale, normalized by the dynamical time

$$\tau_{\text{dyn}} = \sqrt{\frac{3\pi}{32G\rho_{d,\text{avg}}}}, \quad (23)$$

$$= 8.93 \times 10^7 \left(\frac{M_0}{10^9 M_\odot} \right)^{\frac{1}{7}} \text{ yr}, \quad (24)$$

where $\rho_{d,\text{avg}}$ is the mean density of the CDM halo inside r_0 , is given by

$$\frac{\tau_{\text{KH}}}{\tau_{\text{dyn}}} = 24.5 \left(\frac{F}{0.1} \right) \left(\frac{n_{CG}}{10^{-4} \text{cm}^{-3}} \right)^{-1} \times \left(\frac{v_{gal}}{10^3 \text{km s}^{-1}} \right)^{-1} \quad (25)$$

This equation does not have an explicit dependence on the mass of the CDM halo. Massive dwarf galaxies lose the extended gas within $\sim 25\tau_{\text{dyn}}$ for $n_{CG} = 10^{-4} \text{cm}^{-3}$ and $v_{gal} = 1000 \text{km s}^{-1}$. Consequently, we expect that even for the massive dwarf galaxy the extended gas will be stripped through Kelvin-Helmholtz instability within a short time-scale.

On the other hand, Balsara, Livio, & O’Dea (1994) demonstrated that the gas accretes from downstream into the core in their hydrodynamical simulations of the interaction between the ICM and the giant galaxy. Since the dwarf galaxies have shallower potential wells than the giant galaxies, we neglect the effect of the gas accretion from backward into the galaxy. It may play however a role for the massive dwarf galaxies where our estimation of the gas ablation might not be suitable.

4. NUMERICAL MODEL

In addition to the effect of the accretion inflow into the core from downstream, the above analytic arguments neglect the geometrical effects between the gas in dwarf galaxies and the ICM and the presence of the Rayleigh-Taylor instability. Moreover, the compressibility of the gas may become important because the each galaxy moves in the cluster of galaxies with the transonic velocity that is

corresponding to the velocity dispersion of the cluster of galaxies. Therefore, a realistic analysis that uses a hydrodynamic simulation is necessary to examine the effect of the gas removal due to the interaction between a dwarf galaxy and an ICM. In this section, we describe the numerical model of ram pressure stripping from dwarf galaxies.

4.1. Initial conditions and simulation method

For modeling the interaction between a galaxy and an ICM, Portnoy, Pistinner & Shaviv (1993) showed that a treatment of the protons and the electrons as two fluids resulted in negligible differences for the mass of the gas inside the galaxy. In this paper, therefore, the evolution of the gas is described by the hydrodynamic equations for the single perfect fluid. The continuity equation, the momentum equation, and the thermal energy equation are given by

$$\frac{\partial \rho}{\partial t} + \nabla \cdot (\rho \mathbf{v}) = 0, \quad (26)$$

$$\frac{\partial \rho \mathbf{v}}{\partial t} + \nabla \cdot (\rho \mathbf{v} \mathbf{v}) + \nabla P = -\nabla \Phi_d, \quad (27)$$

and

$$\frac{\partial \rho e}{\partial t} + \nabla \cdot (\rho e \mathbf{v}) + \nabla (P \mathbf{v}) = -\rho \mathbf{v} \cdot \nabla \Phi_d, \quad (28)$$

where ρ is the gas density, \mathbf{v} is the gas velocity, P is the gas pressure, $\gamma (= 5/3)$ is the adiabatic index, and e is the total specific energy

$$e = \frac{1}{2} v^2 + \frac{1}{\gamma - 1} \frac{P}{\rho}. \quad (29)$$

Initial conditions are generated using the descriptions in §2. We neglect the effects of the self-gravity of the gas, radiative cooling, the heating by supernovae and stellar winds from massive stars, and the photoionization by ultraviolet radiation background. We discuss them in §5. The equations are solved by a finite difference code VH-1. VH-1 is based on the piecewise parabolic method (PPM)

described by Colella & Woodward (1984) and was written and tested by the numerical astrophysics group at the Virginia Institute for Theoretical Astrophysics. Since the PPM scheme has a great advantage due to the reduction of numerical viscosity, all fluid interfaces are sharply preserved and small-scale features can be resolved. This scheme is, therefore, suited for this class of problems.

The system is assumed to be axial symmetric and described by cylindrical geometry. The center of the fixed gravitational potential given by equation (2) is located on the symmetric axis and the gas distribution of the dwarf galaxy is set up using equation (10). The reflecting boundary condition is adopted at the bottom boundary that corresponds to the symmetric axis and the ICM flows continuously from the left stream boundary parallel to the axis. The outflow boundary conditions, by imposing for each variable a zero gradient ($d/dr = 0$), are adopted at the top and the right stream boundaries. Unfortunately, this condition does not eliminate reflection waves from the boundaries. Thus, the simulation box is separated by two parts such as the inner rectangle $8r_0$ long and $3r_0$ wide and an outer surrounding part to keep the boundaries far away. The grids are equally spaced with 100 zones per core radius for the higher resolution runs or 50 zones for the lower resolution runs in the inner part, and are exponentially spaced in the outer part. A useful additional effect of this non-uniform grid is the increased numerical dissipation of disturbances that propagate to a large distance. This helps solving the problem of residual reflection waves from the boundary.

4.2. Results of simulations

We have performed a parameter study varying the core mass M_0 of the CDM halo from $10^6 M_\odot$ to $10^{10} M_\odot$, varying the relative velocity of the dwarf galaxy v_{gal} from 500 km s^{-1} to 1000 km s^{-1} , and varying the number density n_{CG} of the ICM from 10^{-5} cm^{-3} to 10^{-3} cm^{-3} . Table 1 displays the model parameters of the ICM in this paper.

Figure 2 shows snapshots of the run for the model (c) of $M_0 = 10^7 M_\odot$, $n_{\text{CG}} = 10^{-4} \text{ cm}^{-3}$, and $v_{\text{gal}} = 1000 \text{ km s}^{-1}$ as a function of elapsed time at 5.61×10^6 , 2.86×10^7 , 4.58×10^7 , 7.42×10^7 , and 9.63×10^7 yr. The left and the right colour images show the logarithmic density distribution and the logarithmic pressure distribution, respectively. Arrows in the right panels indicate the velocity vector of the gas flow at each point and their lengths are proportional to the absolute values of their velocity. The CDM halo is located at the origin and the ICM flows in from the left side.

The upper panel shows the early phase of the interaction between the ICM and the gas of the dwarf galaxy. It is clearly seen that the forward shock that propagates through the gas of dwarf galaxy, and the reverse shock that propagates through the ICM are formed in the downstream and the upstream of the contact discontinuity respectively. The propagation of the forward shock causes the strong compression of the gas in the dwarf galaxy as seen in the upper and the second panel. Below the second panel, Kelvin-Helmholtz instabilities are observed at the contact discontinuity.

Since the instabilities are suppressed by the gravity, the growing modes are only the disturbances of the large wave numbers that have the shortest growth time. Disturbances

with small wave numbers grow while moving away from the galaxy. The third panel shows that the gas associated with the dwarf galaxy is accelerated by the ram pressure of the ICM and is pushed out of the potential well. Since the front of the accelerated gas is highly Rayleigh-Taylor unstable, there are many small irregularities in front of the contact discontinuity. Accurately, the feature seen on the symmetric axis ($R = 0$) at $Z \sim 0.5r_0$ is caused by pure Rayleigh-Taylor instability. The combination of Rayleigh-Taylor instability and Kelvin-Helmholtz instability forms other irregularities because the gas flows tangentially to the fluid interface as seen in the third and right panel. However, the perturbations do not grow significantly because the gravity of the CDM halo suppresses Rayleigh-Taylor instability. The gas removal time-scale nicely agrees with the analytical estimate in equation (16) which predicts $\tau_{\text{IS}} = 5.42 \times 10^7$ yr.

Figure 3 shows snapshots of the run for the model (c) of $M_0 = 10^{10} M_\odot$, $n_{\text{CG}} = 10^{-4} \text{ cm}^{-3}$, and $v_{\text{gal}} = 1000 \text{ km s}^{-1}$ as a function of elapsed time at 6.84×10^7 , 6.99×10^8 , 1.15×10^9 , 2.18×10^9 , and 3.26×10^9 yr.

The early evolution of the interaction between the gas and the ICM is almost the same as in the case of $M_0 = 10^7 M_\odot$. However, since the gravitational potential is deep and the central thermal pressure is larger than the ram pressure of the ICM as shown in the analytical model, the mass-loss process is not instantaneous but mild ablation due to Kelvin-Helmholtz instabilities occur. Moreover, the gas interface is Rayleigh-Taylor stable because the gas acceleration is weak. The velocity field in the right bottom panel reveals that the flow turns back and an accretion inflow into the core develops close to the symmetry axis on the downstream side. Accretion occurs quasi-periodically as a radial-pumping mode. The condition of the flow is summarized as follows.

1. This flow from the downstream side and the post-shock gas from the upstream side cause increased compression mainly along the symmetry axis.
2. The gas in the galaxy, therefore, acts by expanding sideways as seen in the third panel. Since this expansion increases the cross section of the interaction between the galactic gas and the ICM, the mass-loss rate increases.
3. The expansion decreases the pressure gradient around the galaxy center and the gas contracts to the galaxy center by the gravitational force. Then the system recovers the quasi-static states again.
4. This cycle repeats again.

This process is effective in the simulations of a massive dwarf galaxy or of a small ram pressure of the ICM. For this specific process, the analytic condition given by §3.2 fails to describe the gas ablation from the dwarf galaxy.

Figure 4 shows the evolution of the gas mass inside the core radius around the center of the dark matter halo as a function of time for core masses of the CDM halo from $10^6 M_\odot$ to $10^{10} M_\odot$. Each curve is categorized by the model parameters (see Table 1). The gas is instantaneously stripped in low-mass dwarfs or for large ram pressures. Due to the accretion inflow into the galactic core from the

down stream, the net mass-loss rate becomes small. Moreover, we can observe oscillations of the total mass inside a core radius due to the mass accretion. These oscillation modes have periods of several dynamical timescales. Even for the massive dwarf galaxy ($M_0 = 10^{10} M_\odot$), the gas could be instantaneously stripped if the ram pressure is large as e.g. in the cores of galactic clusters.

Figure 5 summarizes the results of our simulations. This diagram shows the mass-loss rate due to ram pressure stripping as a sequence of the core mass. Filled circles indicate the cases where the gas in the core radius is completely stripped within 1 Gyr. In these cases the ram pressure stripping by the ICM is very effective and the whole gas in the potential well is rapidly removed. Open circles indicate the cases where the gas in the core radius is not completely stripped within 2 Gyr. In these cases, the ram pressure stripping by the ICM is not so effective. The thin line indicates the relation of

$$\rho_{CG} v_{gal}^2 = \frac{GM_0 \rho_{g0}}{3r_0}, \quad (30)$$

which is the instantaneous stripping condition described in §3.1. This line divides the parameter space into two regions. Stripping is effective for the upper region and is ineffective for the lower region. This relation roughly agrees with the numerical experiments in the range from $M_0 = 10^6 M_\odot$ to $M_0 = 10^{10} M_\odot$. The dashed line indicates the relation of

$$\rho_{CG} v_{gal}^2 = \frac{GM_0 \rho_{g,avg}}{2\pi r_0}, \quad (31)$$

which is the Kelvin-Helmholtz stripping condition described in §3.2. Stripping by Kelvin-Helmholtz instability is effective for the upper region and is not effective for the lower region. Since there is mass accretion from the back of the galaxy, this relation is not well reproduced by the numerical experiments.

Using the data of intermediate cases that are shown by filed triangles in Figure 5, we find a critical core mass for effective ram pressure stripping of

$$M_{cr} = 2.52 \times 10^9 \left(\frac{n_{CG}}{10^{-4} \text{cm}^{-3}} \right)^{\frac{5}{2}} \left(\frac{v_{gal}}{10^3 \text{km s}^{-1}} \right)^5 M_\odot \quad (32)$$

The thick line shows the loci of this critical core mass.

In Figure 5, r_{CG} is the distance from the center of galaxy cluster assuming the isothermal β -model

$$n_{CG} = n_{CG0} \left\{ 1 + \left(\frac{r_{CG}}{r_{CG0}} \right)^2 \right\}^{-\frac{3}{2}\beta}, \quad (33)$$

with $\beta = 0.6$, $n_{CG0} = 2 \times 10^{-3} \text{cm}^{-3}$, $r_{CG0} = 0.25 \text{Mpc}$, and $\sigma_{CG} = 866 \text{km s}^{-1}$, where n_{CG0} and r_{CG0} is the central number density and the core radius of an ICM and σ_{CG} is the line-of-sight velocity dispersion of the galaxy cluster which corresponds to the relative velocity of the dwarf galaxy. If the galaxy number density follows an approximate King model as

$$n_{gal} \propto \left\{ 1 + \left(\frac{r_{CG}}{r_{CG0}} \right)^2 \right\}^{-3/2}, \quad (34)$$

the median radius of the galaxy distribution for $r < 10r_{CG0}$ is about $3.5r_{CG0}$. The shaded region corresponds to ICM conditions inside this radius. The diagram indicates that the process of the ram pressure stripping is very effective for dwarf galaxies in the clusters of galaxies. There, diffuse gas in dwarf galaxies should rapidly be removed.

5. SUMMARY AND DISCUSSION

The physics of the interaction between the ICM and dwarf galaxies confined by a surrounding CDM halo has been studied in detail using analytical estimates and hydrodynamic simulations. We have performed a parameter study varying the core mass of the CDM, the relative velocity of the galaxy and the density of the ICM. We find that the gas in dwarf galaxies is rapidly removed in a typical cluster environment by ram-pressure stripping.

Our results can be applied to clusters of galaxies, where X-ray emission has been observed. Their gas number density n_{CG} at the median radius of the galaxy distribution and the line-of-sight velocity dispersion σ_{CG} are plotted in Figure 6. Data for the central gas density and β are from Jones & Forman (1999) and Briel, Henry & Böhringer (1992), and the velocity dispersions are from the same sources including also Hughes (1989). One particular example, the Coma cluster with $n_0 = 2.89 \times 10^{-3} \text{cm}^{-3}$, $\beta = 0.75$ and $\sigma_{CG} = 1010 \text{km s}^{-1}$, is indicated by a filled circle. Dotted lines are loci of constant M_{cr} given by equation (32) ranging from $10^7 M_\odot$ to $10^{11} M_\odot$. The lines with their various core masses and maximum circular velocities are shown. They indicate that galaxies should rapidly lose all of their diffuse gas by ram pressure stripping. This figure shows that the gas in dwarf galaxies is completely stripped in rich clusters of galaxies within the short time-scale.

The effect of radiative cooling has been neglected in our simulations. we estimate the role of radiative cooling in our models here. Since for low-mass dwarf galaxies ($M_0 \lesssim 10^9 M_\odot$), the ram pressure already exceeds the gravitational force, radiative processes will not be able to affect the gas stripping. However, it might play a role for massive dwarf galaxies ($M_0 \gtrsim 10^9 M_\odot$) which have deeper potential wells. The cooling time-scale is defined as (Efstathiou 1992)

$$\tau_{cool} = \frac{3}{2} \frac{1}{\mu^2 (1-Y)^2} \frac{k_B T}{n_g \Lambda}, \quad (35)$$

where $Y (= 0.25)$ is the helium mass fraction, n_g is the gas number density, and Λ is cooling rate. If we evaluate this time-scale for our standard model $M_0 = 10^9 M_\odot$ using conditions immediately behind the leading shock, we find that $\tau_{cool} = 3.18 \times 10^9 \text{yr}$ assuming $T = 10^7 \text{K}$, $\Lambda = 10^{-23} \text{erg s}^{-1} \text{cm}^{-3}$, and $n_g = 1.0 \text{cm}^{-3}$ from the result of our simulations. This time-scale is larger than the instantaneous stripping time-scale ($\tau_{IS} = 2.03 \times 10^8 \text{yr}$) that is given by equation (16). This implies that gas stripping from the massive dwarf galaxies is affected by the radiative cooling.

However, we would then also need to consider the effects of the star formation and subsequent feedback process such as stellar winds and supernovae heating from

massive stars. These feedback processes supply thermal energy to the gas and prevent efficient cooling (Dekel & Silk 1986; Mori et al. 1997; Mori et al. 1999). In addition, the photoionization due to the ultraviolet background radiation prevents gas cooling and keeps the gas hot (Efstathiou 1992; Babul & Rees 1992). Furthermore, though we studied only the interaction between the ICM and a hot interstellar medium in this paper, it is very interesting to examine also the fate of the cool and dense interstellar medium in a dwarf galaxy. In this case, the stripping history of the gas may be quite different even for the less-massive dwarf galaxies ($M < 10^9 M_\odot$). In a series of forthcoming studies, we will report the results of taking into account the multi-phase states of the gas with cool components in a galaxy, including the effect of the radiative cooling of the gas, energy input from stars, and the ultraviolet background radiation.

We conclude that the ram pressure stripping of the diffuse gas from dwarf galaxies by the ICM is of prime importance to understand the morphology-density relation for dwarf galaxies and the chemical evolution of dwarf galaxies. Most of the heavy elements ejected by massive stars through Type II supernovae are found in the warm and hot diffuse gas. In order for these heavy elements to be incorporated into stars, the hot gas has to cool and form cold clouds again. Our models indicate that this will be impossible for dwarf galaxies in clusters of galaxies, as the gas is stripped before condensing into clouds. Ram pressure stripping therefore plays a significant role for the chemical evolution of dwarf galaxies. Our results imply that most of the chemical evolution of dwarf galaxies must have occurred at high redshift, before the virialized cluster had formed.

This work has been supported in part by the Research Fellowship of the Japan Society for the Promotion of Science for Young Scientists (6867) of the Ministry of Education, Science, Sports, and Culture in Japan. M.M. would like to thank the Max-Planck-Institut für Astronomie for its hospitality throughout this research. Numerical calculations were carried out at Max-Planck-Institut für Astronomie in Germany and at the Astronomical Data Analysis Center of the National Astronomical Observatory in Japan.

REFERENCES

- Babul, A., & Rees, M. 1992, MNRAS, 255, 346
 Balsara, D., Livio, M., & O'Dea, C.P. 1994, ApJ, 437, 83
 Binggeli, B., Tammann, G., & Sandage, A. 1987, ApJ, 94, 251
 Binggeli, B., Tarengi, M., & Sandage, A. 1990, A&A, 228, 42
 Böhringer, H., Nulsen, P.E., Braun, R., & Fabian, A.C. 1995, MNRAS, 274, L67
 Briel, U.G., Henry, J.P., & Böhringer, H. 1992, A&A, 259, L31
 Burkert, A. 1995, ApJ, 447, L25
 Burkert, A., & Ruiz-Lapuente, P. 1997, ApJ, 480, 297
 Chandrasekhar, S. 1961, *Hydrodynamic and Hydromagnetic Stability* (Oxford:Oxford University Press)
 Cole, S., Aragón-Salamanca, A., Frenk, C.S., Navarro, J.F., & Zepf, S.E., 1994, MNRAS, 271, 781
 Colella, P., & Woodward, P. 1984, JCP, 54, 174
 Dekel, A., & Silk, J. 1986, ApJ, 303, 39
 Dressler, A. 1980, ApJ, 236, 351
 Dubinski, J., & Carlberg, R. 1991, ApJ, 378, 496
 Efstathiou, G. 1992, MNRAS, 256, 43P
 Ferguson, H., & Sandage, A. 1988, AJ, 96, 1520
 Flores, R.A., & Primack, J.R. 1994, ApJ, 427, L1
 Fukushige, T., & Makino, J. 1997, ApJ, 477, L9
 Hughes, J.P. 1989, ApJ, 337, 21
 Ikeuchi, S., 1986, Ap&SS, 118, 509
 Irwin, J.A., Seaquist, E.R., Taylor, A.R., & Duric, N. 1987, ApJ, 313, L91
 Jones, C., & Forman, C. 1999, ApJ, 511, 65
 Katz, N., Weinberg, D.H., & Hernquist, L., 1996, ApJS, 105, 19
 Moore, B. 1994, Nature, 370, 629
 Moore, B., Governato, F., Quinn, T., Stadel, J., & Lake, G. 1998, ApJ, 499, L5
 Mori, M., Yoshii, Y., & Nomoto, K. 1999, ApJ, 511, 585
 Mori, M., Yoshii, Y., Tsujimoto, T., & Nomoto, K. 1997, ApJ, 478, L21
 Murray, S.D., White, S.D.M., Blondin, J.M., & Lin, D.N. 1993, ApJ, 407, 588
 Navarro, J.F., Frenk, C.S., & White, S.D.M. 1996, ApJ, 462, 563
 Navarro, J.F. & Steinmetz, M., 1997, ApJ, 478, 13
 Nulsen, P.E.J. 1982, MNRAS, 198, 1007
 Portnoy, D., Pistinner, S., & Shaviv, G. 1993, ApJS, 86, 95
 Rees, M.J., 1986, MNRAS, 218, 25p
 Thuan, T.X., Alimi, J.M., Gott, J.R., & Schneider, S.E. 1991, ApJ, 370, 25
 White, D.A., Fabian, A.C., Forman, W., Jones, C., & Stern, C. 1991, ApJ, 375, 35
 White, S.D.M. & Frenk, C.S., ApJ, 379, 52
 Yoshii, Y., & Arimoto, N., 1987, A&A, 188, 13

FIG. 1.— The density (upper) and the circular velocity (lower) of the Burkert's (1995) profile. Each curve is divided by the core mass of the dark matter halo which ranges from $10^6 M_\odot$ (left) to $10^{10} M_\odot$ (right).

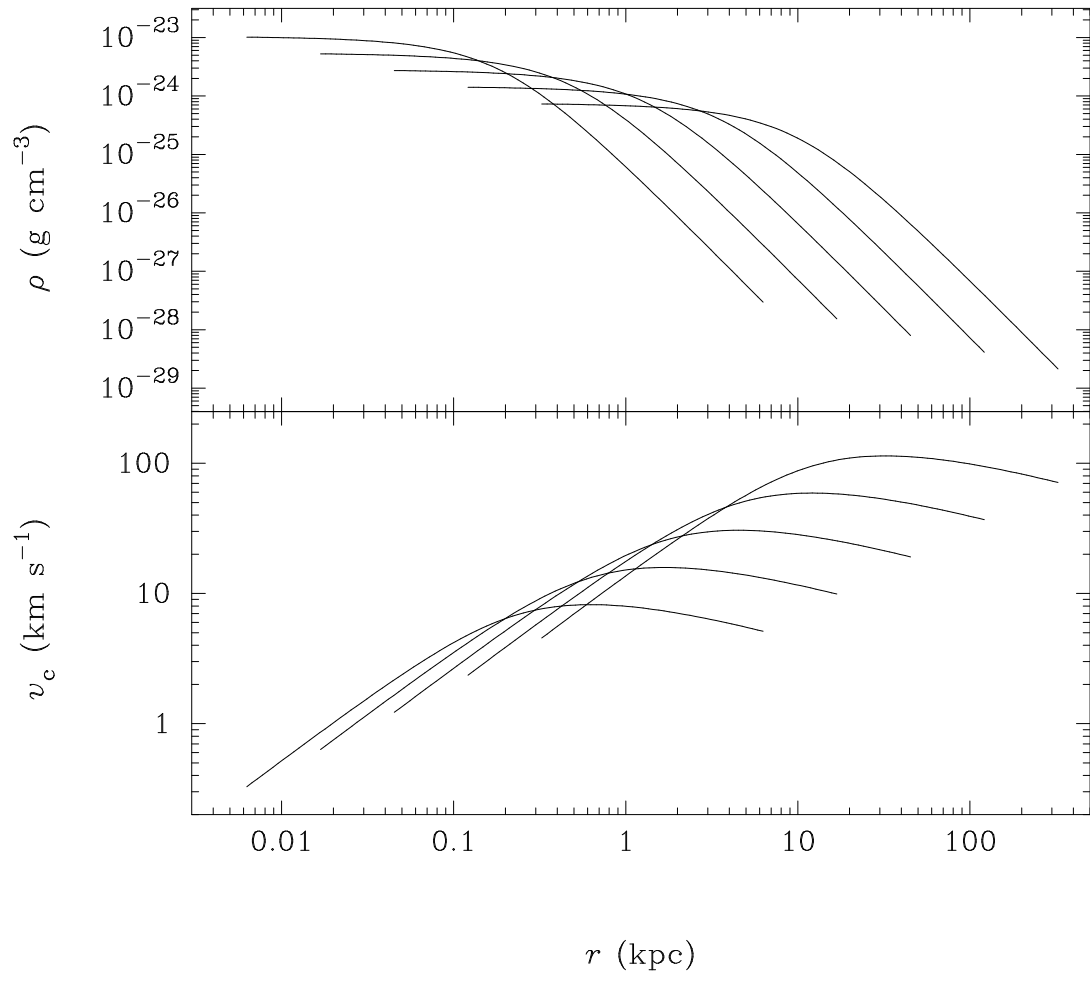
FIG. 2.— Snapshots for the model with core mass $M_0 = 10^7 M_\odot$, number density of the ICM $n_{CG} = 10^{-4} \text{ cm}^{-3}$, and relative velocity of the galaxy $v_{gal} = 1000 \text{ km s}^{-1}$ as a function of elapsed time at 5.61×10^6 , 2.86×10^7 , 4.58×10^7 , 7.42×10^7 , and $9.63 \times 10^7 \text{ yr}$. The left and the right colour images show the logarithmic density distribution and the logarithmic pressure distribution, respectively. Arrows in the right panels indicate the velocity vector of the gas flow at each point.

FIG. 3.— Snapshots for the model with core mass $M_0 = 10^{10} M_\odot$, number density of the ICM $n_{CG} = 10^{-4} \text{ cm}^{-3}$, and relative velocity of the galaxy $v_{gal} = 1000 \text{ km s}^{-1}$ as a function of elapsed time at 6.84×10^7 , 6.99×10^8 , 1.15×10^9 , 2.18×10^9 , and $3.26 \times 10^9 \text{ yr}$. The left and the right colour images show the logarithmic density distribution and the logarithmic pressure distribution, respectively. Arrows in the right panels indicate the velocity vector of the gas flow at each point.

FIG. 4.— The evolution of the gas mass inside the core radius of the gravitational potential of the CDM halo as a function of time. Each column corresponds to a core mass of the CDM halo which varies from $10^6 M_\odot$ to $10^{10} M_\odot$. Each curve is categorized by the model parameters (dash-dot-dot-dotted line: $n_{CG} = 10^{-3} \text{ cm}^{-3}$ and $v_{gal} = 1000 \text{ km s}^{-1}$, dotted line: $n_{CG} = 10^{-3} \text{ cm}^{-3}$ and $v_{gal} = 500 \text{ km s}^{-1}$, dash-dotted line: $n_{CG} = 10^{-4} \text{ cm}^{-3}$ and $v_{gal} = 1000 \text{ km s}^{-1}$, dashed line: $n_{CG} = 10^{-4} \text{ cm}^{-3}$ and $v_{gal} = 500 \text{ km s}^{-1}$, and solid line: $n_{CG} = 10^{-5} \text{ cm}^{-3}$ and $v_{gal} = 1000 \text{ km s}^{-1}$). Each horizontal line indicates the time scale of $10\tau_{dyn}$.

FIG. 5.— The mass loss time-scale for dwarf galaxies as a result of ram pressure stripping $\rho_{CG} v_{gal}^2$ due to the ICM as a sequence of the core mass M_0 and the maximum circular velocity $v_{c,max}$ of dwarf galaxies. Filled circles indicate the case that the gas is stripped within 1 Gyr. Open circles show that the gas is not stripped within 2 Gyr. Intermediate cases are marked by filled triangles. The shaded region corresponds to the inside of the median radius of the galaxy distribution for a typical galaxy cluster fitted by β -model $n_{CG} = n_{CG0} \{1 + (r_{CG}/r_{CG0})^2\}^{-3\beta/2}$, with $\beta = 0.6$, the central number density $n_{CG0} = 2 \times 10^{-3} \text{ cm}^{-3}$, the core radius $r_{CG0} = 0.25 \text{ Mpc}$, and the line-of-sight velocity dispersion $\sigma_{CG} = 866 \text{ km s}^{-1}$. r_{CG} is the distance from the center of cluster.

FIG. 6.— A scaled gas density is plotted against velocity dispersion for clusters of galaxies. Assuming a distribution of the gas that follows the β -model, the gas number density is given at the median radius of the galaxy distribution. Data for the central gas density and β are from Jones & Forman (1999) and Briel, Henry & Böhringer (1992), and the velocity dispersions are from these sources and from Hughes (1989). The filled circle corresponds to the Coma cluster. Solid lines are loci of constant M_{cr} which is the critical core mass of the CDM halo, and the lines are labeled with their core mass and the maximum circular velocity. The lines indicate that dwarf galaxies should lose instantaneously all of their gas by ram pressure stripping.



This figure "f2.jpg" is available in "jpg" format from:

<http://arxiv.org/ps/astro-ph/0001422v1>

This figure "f3.jpg" is available in "jpg" format from:

<http://arxiv.org/ps/astro-ph/0001422v1>

